Experimental Mechanics (2006) 46: 205–216
DOI 10.1007/s11340-006-6418-4

Particle Velocimetry and Photoelasticity Applied to the Study of Dynamic Sliding Along Frictionally-Held Bimaterial Interfaces: Techniques and Feasibility

G. Lykotrafitis · A.J. Rosakis · G. Ravichandran

Received: 3 August 2005 / Accepted: 21 November 2005

Abstract A laser interferometry-based technique was developed to locally measure the in-plane components of particle velocity in dynamic experiments. This technique was applied in the experimental investigation of dynamic sliding along the incoherent (frictional) interface of a Homalite–steel bimaterial structure. The bimaterial specimen was subjected to uniform compressive stress and impact-induced shear loading. The evolution of the dynamic stress field was recorded by high-speed photography in conjunction with dynamic photoelasticity. The combination of the full-field technique of photoelasticity with the local technique of velocimetry was proven to be a very powerful tool in the investigation of dynamic sliding. A relatively broad loading wave with an eye-like structure emanated from the interface. The particle velocity measurements established that sliding started behind the eye-like fringe pattern. It propagated with supershear speed with respect to Homalite. A shear Mach line originating from the sliding tip is visible in the photoelastic images. A vertical particle velocity measurement revealed the existence of a wrinkle-like pulse traveling along the bimaterial interface. The wrinkle-like pulse followed the initial shear rupture tip and propagated at a specific subshear speed.

Keywords Dynamic frictional sliding · Incoherent interface · Bimaterial system · Photoelasticity · In-plane velocity measurement · Supershear rupture · Subshear wrinkle-like pulse

G. Lykotrafitis (✉, SEM member) · A.J Rosakis (SEM member) · G. Ravichandram (SEM member)
California Institute of Technology, California, USA
e-mail: gcl@its.caltech.edu

Introduction

The measurement of the in-plane components of particle velocity is a challenging problem in experimental mechanics and only a few attempts have been made to address it [14–18]. In this paper, a relatively simple, but very accurate, technique is introduced for measuring the in-plane (horizontal and vertical) and the out-of-plane components of particle velocity in dynamic experiments. After the technique is established, it is applied to the investigation of dynamic sliding along incoherent (frictionally-held) interfaces of bimaterial systems.

Earlier interest on dynamic failure processes along bimaterial interfaces has been focused on the case of coherent interfaces (bonded interfaces of finite strength and toughness). However, many composite structures in various engineering applications (e.g., bolted joints and sandwich structures) consist of layers of different materials held together by applied pressure without any bond between the contact faces. In order to utilize these layered structures effectively, the failure process along their incoherent interfaces is the key problem to be investigated. Here, we confine our attention to the failure process generated by impact shear loading. Unlike the case of coherent interfaces, where the resistance to failure through sliding is related to the strength and toughness of the bond between the plates, in the incoherent case the resistance to sliding comes from the frictional stresses between the surfaces in contact.

There are two approaches to describing frictional sliding. The most classical approach uses elastodynamic shear crack models (behind the leading edge of

sliding, the surfaces slide continuously and interact through contact and friction). More recently, models that describe sliding as 'self-healing' slip pulse have been introduced (behind the leading edge of the sliding, there is sliding for a finite length followed by surface locking).

Classic dynamic fracture theories [1, 2] of growing shear cracks have many similarities to the frictional sliding process. These theories treat the rupture front as a distinct point (sharp-tip crack). The crack-like rupture of coherent interfaces, separating similar and dissimilar solids subjected to dynamic shear loading, has been the subject of extensive experimental, numerical and analytical investigations in the past years and was summarized by Rosakis [3] in a recent review. Of relevance to the present study is the persistent occurrence of intersonic shear rupture along coherent bimaterial interfaces [4–9].

Theoretical and numerical investigations [10–12] have shown that incoherent interfaces of compressed bimaterial structures can sustain interface waves involving separation (wrinkle-like pulses). Particle displacement in a direction perpendicular to the interface is greater in the slower material than in the faster material; that may result in a local separation of the interface during sliding. Wrinkle-like pulses have also been observed experimentally in rubber sliding experiments [13]. We note that the wrinkle-like pulses propagate at a speed between the Rayleigh wave speed and the shear wave speed of the slower material and are different from the Schallamach waves which are very slow compared to the wave speeds of the involved materials.

In this paper, laser interferometry-based velocimetry is combined with dynamic photoelasticity to record frictional sliding events at incoherent interfaces of bimaterial systems in a microsecond time scale. Pairs of rectangular Homalite and steel plates are used. A uniform external compressive stress is applied to the bimaterial specimen via a hydraulic press. Asymmetric impact loading is imposed using a gas gun and a steel projectile. The fringe pattern evolution in conjunction with the sliding velocity history gives direct evidence of the sliding mode, the existence of a supersonic disturbance with respect to Homalite, the exact point of sliding initiation and the sliding propagation speed. Strong evidence of a wrinkle-like pulse traveling along the interface is also recorded. The results presented here show that under certain loading conditions the failure of bimaterial structures subjected to impact shear loading can take the form of a supershear crack-like sliding, followed by a local opening displacement in the form of a wrinkle-like pulse.

Materials and Specimen Configuration

Experiments were performed to investigate the nature of dynamic frictional sliding along the incoherent interface of a high-contrast bimaterial system. The bimaterial specimen consisted of a Homalite-100 plate and a steel plate held together by a uniform compressive stress [see Fig. 1(a)]. Homalite-100 is a mildly rate-sensitive brittle polyester resin that exhibits stress-induced birefringence with an optical coefficient $F_\sigma = 22.6KN/m$. At the strain rate developed during the experiments (on the order of $10^3\ s^{-1}$) and at room temperature, Homalite exhibits a purely linear elastic behavior. The longitudinal, shear and Rayleigh wave speeds in Homalite are $C_1^H = 2583\ m/s$, $C_2^H = 1249\ m/s$ and $C_R^H = 1155\ m/s$ respectively. Steel was chosen as the other half of the bimaterial system because it provides a strong material property mismatch across the interface, similar to mismatches encountered in composites. The dilatational, shear and Rayleigh wave speeds in steel are $C_1^S = 5838\ m/s$, $C_2^S = 3227\ m/s$ and $C_R^S = 2983\ m/s$ respectively. The wave speeds for Homalite and steel were obtained by ultrasonic measurements using shear and pressure transducers operating at 5 MHz.

In the experiments, the configuration was approximated by plane stress conditions, since plate specimens

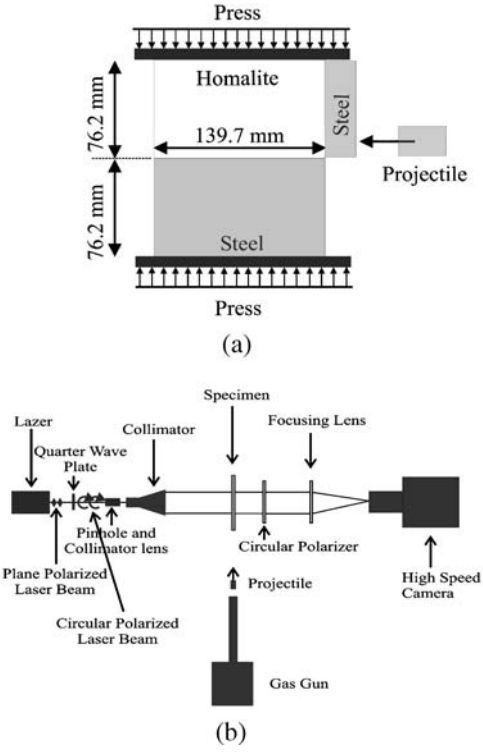

Fig. 1. (**a**) Geometry and loading configuration for a bimaterial specimen consisting of a Homalite and a steel plate. (**b**) Dynamic photoelasticity setup

76.2 *mm* high, 139.7 *mm* long and 9.525 *mm* thick were employed. The shear wave speeds are identical in 3-D and for the plane stress approximation. The same is true for the Rayleigh wave speed, since the contribution in the Rayleigh wave formation comes primarily from the shear wave. However, the plane stress longitudinal wave speeds of Homalite-100 and steel are $C_{1\sigma}^{H} = 2187\,m/s$, $C_{1\sigma}^{S} = 5378\,m/s$ respectively.

Experimental Setup and Procedure

A combination of two experimental techniques was used in this investigation. Dynamic Photoelasticity, which gives the full field maximum shear stress distribution, was used in conjunction with a new technique based on laser interferometry. This technique provides a continuous local measurement of the horizontal and vertical components of the relative velocity of two adjacent points across the bimaterial interface. The initiation and evolution of sliding was explored through photoelasticity and velocimetry at a microsecond time scale.

The compressive stress was applied with a press calibrated using a load cell. The asymmetric impact loading was imposed via a cylindrical steel projectile with a diameter of 25 *mm* and a length of 51 *mm*, fired by a gas gun. A steel buffer 73 *mm* high, 25.4 *mm* long and 9.525 *mm* thick was attached to the impact side of the Homalite plate to prevent shattering and to induce a more or less planar loading wave.

Dynamic Photoelasticity Setup

A typical experimental setup for dynamic photoelasticity experiments is shown in Fig. 1(b). The optical setup was arranged for a light field. Isochromatic fringes are contours of maximum in-plane shear stress τ_{max} governed by the stress optical law

$$2\tau_{max} = \sigma_1 - \sigma_2 = NF_\sigma/h$$

where F_σ is the material's stress optical coefficient, h is the specimen thickness, σ_1, σ_2 are the principal stresses and $N = n + 1/2$ (with $n = 0, 1, 2, \ldots$) is the isochromatic fringe order. A continuous laser was used as the light source in our experiments. The laser was set to operate on a single wave length of 540 *nm* (green light). It emitted an intense beam of 2 *mm* in diameter and 100:1 vertically polarized. The laser beam first passed through a quarter wave plate, which transformed it into a circular polarized beam. Then it passed through a 6 μm pinhole and a collimator lens. Finally, the coherent monochromatic circular polarized light went through a collimator lens and expanded in a uniform laser beam of 130 *mm* diameter. The laser beam was transmitted through the specimen and an analyzer. The resulting photoelastic fringe pattern was recorded with a high-speed digital camera (Cordin model 220), which is able to record 16 distinct frames at framing rates up to 100 million frames per second. In this experimental work, most of the high-speed photography was performed at 250,000 to 1,000,000 frames per second. The field of view was wide enough to cover most of the specimen.

Sliding Velocity Measurement Setup

The local sliding velocity was obtained as follows. A pair of fiber-optic velocimeters measured the horizontal particle velocities at two adjacent points across the interface. The horizontal relative velocity history was obtained by subtracting the velocity of the lower plate point from the velocity of the upper plate point. A schematic representation of the setup is shown in Fig. 2(a). The laser beams emitted from the velocimeter heads were focused on points M_1 and M_2 on the thin vertical surfaces of the reflective membranes, which were attached to the surfaces of the Homalite

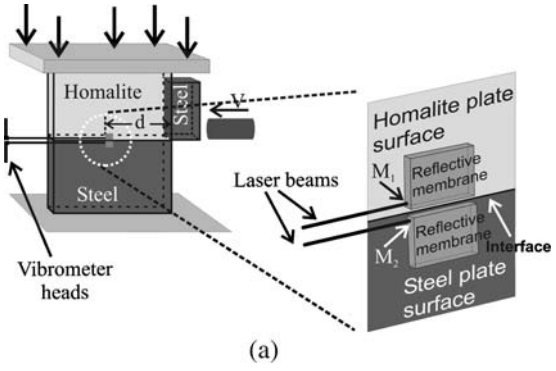

Fig. 2. (**a**) Schematic illustration of the experimental configuration for the sliding velocity measurement. The area inside the dotted line is shown magnified. (**b**) Photograph of the actual setup

(top) and steel (bottom) plates respectively. The distance of each point from the interface was less than 250 μm before compression, and both points had the same horizontal distance from the impact side of the Homalite plates. A picture of the actual setup is presented in Fig. 2(b). The velocimeter and its use in measuring the in-plane components of a particle velocity are described in detail in the next section.

Simultaneous Measurement of the Horizontal and Vertical Components of the Velocity

We can also use the two velocimeters, to measure not only the horizontal component of the in-plane velocity, but the vertical component as well. For this, the laser beam is aimed perpendicular to the narrow horizontal surface of the reflective membrane. Preliminary experimental results showed that the velocities in steel plate are one order of magnitude slower than the velocities in Homalite plate. Taking advantage of this fact, we assumed that particle velocities in the steel were negligible and we carried out several tests using the two velocimeters we had at our disposal (velocimeters 1 and 2 in Fig. 3) to record both the horizontal and vertical in-plane particle velocities. These were subsequently interpreted as sliding and opening speeds respectively. A schematic of the setup used for the measurement is shown in Fig. 3.

Particle Velocity Measurement Setup

As described previously, the slip velocity measurement involved a pair of independent fiber-optic velocimeters that continuously measured the horizontal particle velocities at two adjacent points across the interface.

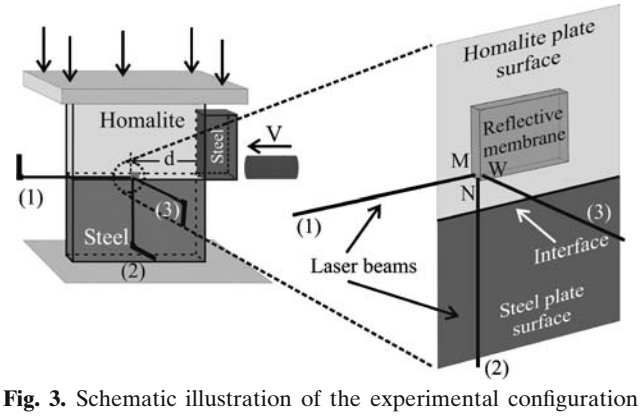

Fig. 3. Schematic illustration of the experimental configuration for the simultaneous measurement of the components of the particle velocity. The area inside the dotted line is shown magnified

By subtracting the velocity of the point below the interface from that of the point above the interface, the horizontal relative velocity history was obtained. Since this is the first time the technique of the in-plane relative velocity measurement is presented, different issues that emerged during its development are addressed. We start by describing a relatively simple yet very accurate method to measure the in-plane and the out-of-plane components of the velocity at one point in the top plane. A point worth noting is that there have been only a few attempts to obtain in-plane particle velocities associated with classical fracture mechanics [14–18].

A velocimeter was used to measure the horizontal and vertical in-plane components of the particle velocity as well as the out-of-plane velocity component. The velocimeter is composed of a modified Mach-Zehnder heterodyne interferometer (Polytec, OFV-511) and a velocity decoder (Polytec, OFV-5000). The interferometer combines the reference beam, which undergoes modulation through a Bragg cell, with the reflected beam from the surface point where the particle velocity is measured. From the interference of these two beams, the decoder gives the component of the velocity along the direction of the laser beam. The decoder was set to a full range scale of ± 10 m/s with a maximum frequency of 1.5 MHz and a maximum acceleration of 10^7 g. The beam spot size was approximately 70 μm, whereas the error of the velocity measurements was 1%.

Figure 3 shows how the different components of the particle velocity were measured. A reflective membrane 360 μm thick was attached to the surface. For the measurement of the out-of-plane component of the particle velocity, the velocimeter laser beam had to be perpendicular to the surface of the reflective membrane at the measurement position (beam 3 in Fig. 3 focused at W). For the measurement of the in-plane horizontal component of the velocity, the laser beam had to be horizontal, parallel to the specimen surface, and focused on the vertical lateral surface of the membrane (beam 1 in Fig. 3 focused at M). The vertical component of the velocity was measured by the vertical beam (beam 2 in Fig. 3 focused at N) which was perpendicular to the horizontal lateral surface of the membrane. The reflective membrane consisted of small glass spheres (approximately 50 μm in diameter) that were glued with an elastic epoxy to the plate surface. Each sphere acts as a small 'cat's-eye', scattering light back along the path of the incident beam. As the laser beam usually hits several glass beads at one time, each of the beams can interfere with each other and produce a speckle

pattern. If the focused spot is very small, as it was in the presenting experiments, the number of scattering centers is small and the angular dependence of the path length differences in a given direction is also small. This leads to a large solid angle over which the interference condition is reasonably constant and the speckle noise is small. In the experiments, the deviation of the laser beams from the normal direction to the corresponding membrane surface was approximately 2° to 3°, and an excellent quality signal was received from the velocimeter. This amount of deviation angle did not affect the results, as we demonstrate below.

Reliability of the Proposed Technique

As previously mentioned, two independent velocimeters were employed in the experiments. We first verified that both instruments were calibrated. To this end, we simultaneously measured the out of plane component of the velocity of the same point by the two velocimeters. Both instruments gave exactly the same result.

Another issue to be clarified is the following. The velocimeter measures the component of the velocity of a point at the thin lateral surface of the reflective membrane along the direction of the laser beam. In order to prove that the velocity of the point on the membrane and the velocity of the corresponding point on the plate were the same, the following comparison was performed. Two reflective membranes were attached to the edge of the Homalite plate, on the side opposite the impact position [see Fig. 4(a)]. One was attached to the narrow surface S_1, which was perpendicular to the direction of the impact, and the second membrane was attached to the lateral surface S_2, which was parallel to the direction of impact. The horizontal particle velocities were measured at points A and B. The distance between these two points was approximately 2 *mm*. The laser beam that was focused at A was vertical to the large membrane surface, and the out-of-plane velocity with respect to plane S_1 was measured. This is the most favorable arrangement for the instrument, since it has been designed to measure the out-of-plane velocities. We note that the above measurement gives the velocity of a point on the plate. The laser beam focused on B was vertical to the narrow surface of the membrane, and it measured the horizontal in-plane component of the velocity at point B of the membrane. Since point A was very close to point B, we can argue that their velocities should also be very similar. The confining pressure was 10 *MPa* and the impact speed 11 *m/s*. In Fig. 4(b), the velocity histories of both points A and B are shown. In this case the distance from the measurement points to the interface was $d = 5$ *mm*, and both instruments gave almost identical results. The wave front arrived at the measurement points simultaneously at around 100 μ*s*. The particle velocity increased until it reached a maximum value of approximately 7 *m/s*, and then it decelerated. Since the devices gave very similar results, we can safely argue that the point on the membrane had the same speed as the most adjacent point on the plate's surface. Thus, we conclude that the procedure we followed for the measurement of the in-plane component of the velocity was accurate.

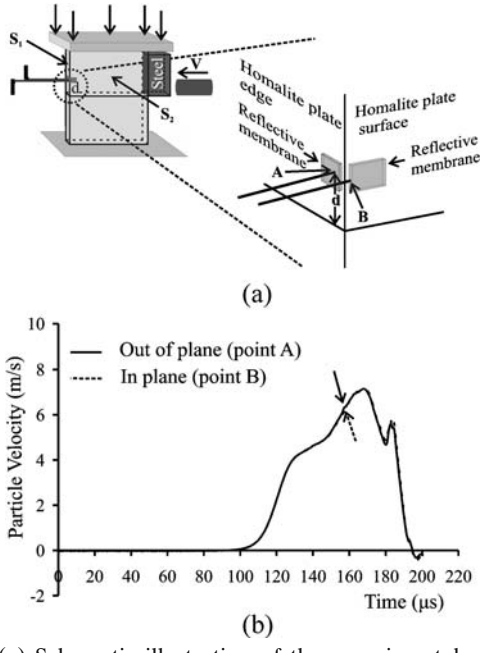

Fig. 4. (**a**) Schematic illustration of the experimental setup for the out-of-plane (A) and in-plane (B) horizontal particle velocity measurement. (**b**) Histories of the out-of-plane and in-plane horizontal particle velocities

The final subject for investigation is the following. In order to measure the horizontal component of the particle velocity at a point on the surface, the laser beam had to be horizontal and parallel to the plate surface. The maximum difference between the height of the velocimeters' heads and the height of the point of reflection was less than 2.5 *mm*. It is also noted that the velocimeters' heads were at a distance of about 300 *mm* from the side of the reflective membrane. A difference in height of 2.5 *mm* results in a deviation angle from the horizontal direction of less than 0.5°. This small deviation did not affect our measurements, since the error from the projection of the velocity on the laser beam is two orders of magnitude less than the intrinsic error of the velocimeter, which is 1%.

Although the deviation from the horizontal direction was very small, we were sometimes forced to move the velocimeter head a small distance out of the vertical plane of the specimen in order to have a good quality signal. The maximum angle was 2.5°, and in order to be sure that this lateral deviation did not affect the results, the following experiment was performed. A uniform compressive stress 10 *MPa* was applied on a bimaterial (Homalite-steel) specimen. A reflective membrane was attached to the surface of the Homalite plate. Two independent velocimeters were pointed at essentially the same point A on the reflective membrane, but in different angles with respect to the vertical plane [see Fig. 5(a)]. Point A was at a distance of 70 *mm* from the impact side of the Homalite plate and 25 *mm* from the interface. One laser beam formed an angle of approximately 1° with the vertical plane, and the other laser beam formed an angle of approximately 5°. The distance of the velocimeter head from the measurement point was approximately 300 *mm*. A projectile hit the buffer at a speed of 9.5 *m/s*. The diagram in Fig. 5(b) illustrates the variation of the component of the horizontal particle velocity at A along the directions of the laser beams of the two different velocimeters. Both measurements were almost identical, and we conclude that even a 5° deviation angle from the vertical plane did not affect the result. It is noted that 5° is a very large deviation angle since it corresponds to a 25 *mm* translation of the velocimeter head out of the plane of the Homalite plate, and it never happened during the frictional sliding experiments. After the above tests, we concluded that the experimental error, due to small misalignments of the laser beam, was smaller than the inherent velocimeter error of 1%.

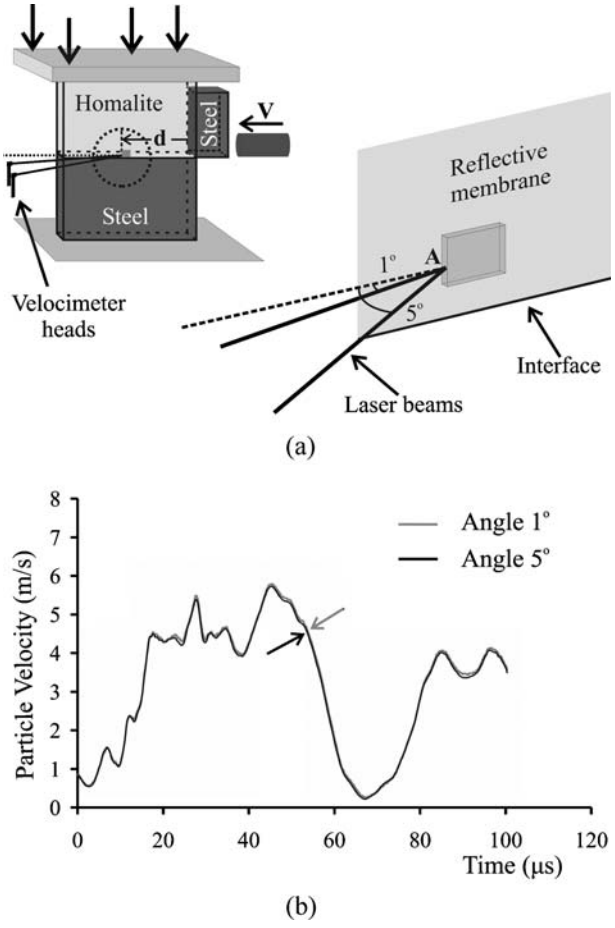

Fig. 5. (**a**) Schematic illustration of the experimental setup for the horizontal particle velocity measurement for angles of 1° and 5° between the laser beam and the vertical Homalite plane. (**b**) Histories of the horizontal particle velocity for angles of 1° and 5° between the laser beam and the vertical Homalite plane. The point A was at a distance $d = 70$ *mm* from the impact side of the Homalite plate

The results of the above investigation demonstrate that the measurement technique can be used with confidence to record, in real time, the in-plane components of the particle velocity on the surface of a plate.

Experimental Results

Initiation and Evolution of Dynamic Frictional Sliding

In the present experiments, dynamic photoelasticity (in conjunction with high-speed photography) was combined with velocimetry to investigate the initiation and evolution of frictional sliding along the incoherent interface of a bimaterial consisting of Homalite and steel. The specimen was subjected to a uniform compressive load of 10 *MPa* and impacted on the Homalite side at a speed of 16.5 *m/s*.The sequence of photoelastic images in Fig. 6 is studied in combination with the horizontal velocities measurements presented in Fig. 7. The images in Fig. 6 show the isochromatic fringe pattern in the Homalite plate at selected times. A pair of fiber-optic velocimeters recorded the history of the horizontal in-plane velocities of two adjacent points, M_1 and M_2 in the Homalite (top) and steel (bottom) plate respectively (see Fig. 2). Both points were at the same horizontal distance of 110 *mm* from the impact side of the Homalite plate and at less than 250 μm from the interface. Figure 7 shows the histories of the horizontal in-plane velocities of both points, as well as the history of the relative horizontal velocity. The insert in Fig. 7(a) shows the history of the relative displacement.

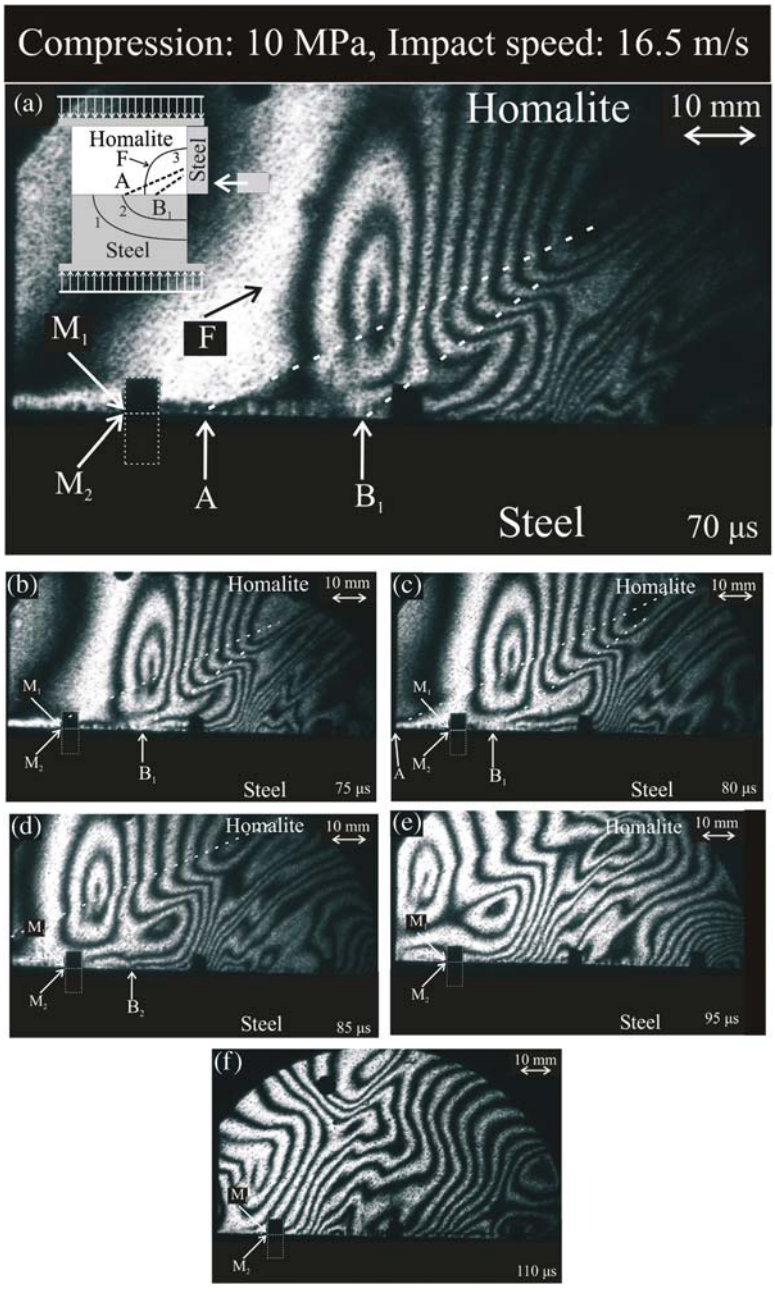

Fig. 6. A sequence of isochromatic fringe patterns showing an intersonic frictional sliding, the corresponding shear Mach line (B) and a shear head wave (A). M_1 and M_2 are the positions of the velocity measurements

The images in Fig. 6(a)–(e) have a similar structure, and this signifies that sliding had reached a more or less steady state. At 110 μs [see Fig. 6(f)], reflected waves from the free left side of the plate had entered the picture and the sliding process became transient, resulting in a distorted photoelastic fringe pattern. As can be seen in Fig. 6(a), the compressive stress wave (P-wave) in the Homalite plate arrives from the right, in front of a relatively broad fringe structure (shown just behind point F), which has a rib-eye structure and emanates from the interface. Since this structure was missing in similar experiments, without external pressure, we conjecture that it was caused by the interference of the impact wave with the preexisting static pressure.

A head wave emanates from point A on the interface and crosses the eye-like fringe structure. Point A is ahead of the P-wave front in the Homalite plate. This shows that a disturbance was traveling along the interface at a speed higher than the P-wave in Homalite. The propagation speed V of the disturbance A was obtained by two different methods and found to

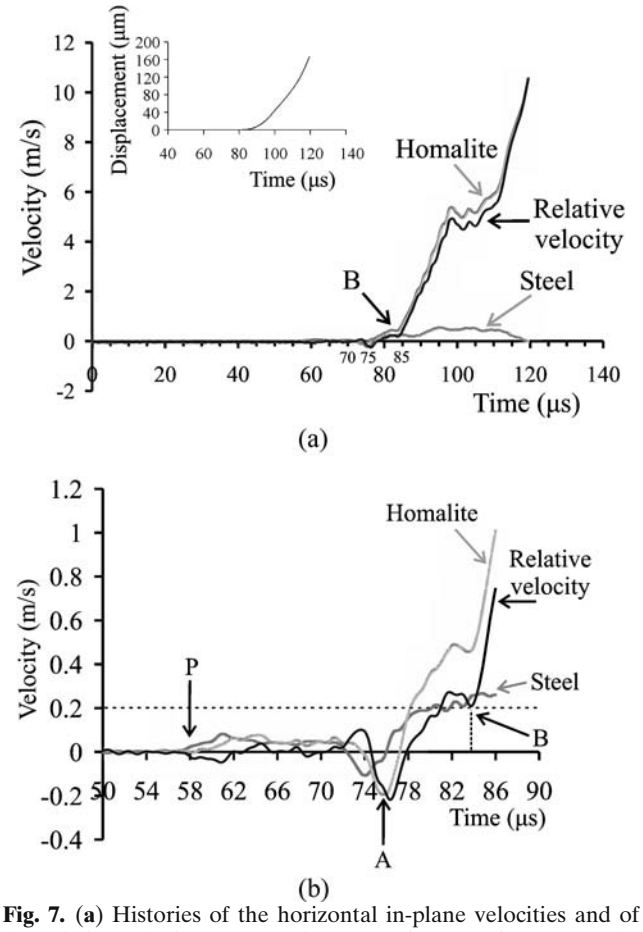

Fig. 7. (**a**) Histories of the horizontal in-plane velocities and of the relative velocity, measured at two adjacent points across the interface at 110 *mm* from the impact side of the Homalite plate. The sliding initiated at B. The insert shows the history of the relative displacement (**b**) Detail of the velocity history diagram, showing the arrival of the P-wave front in the steel plate (P), the arrival of the shear wave front in the steel plate (A) and the sliding initiation (B)

be constant. First, we followed the positions of point A in different frames (Fig. 8). The variation is very well approximated as linear and thus we can conclude that the propagation speed was constant. A linear interpolation gave a traveling speed of 2923 $m/s = 2.13C_1^H = 0.9C_2^S = 0.98C_2^R$, where C_1^H is the P-wave speed of Homalite, C_2^S is the shear wave speed of steel and C_R^S is the Raleigh wave speed of steel. Then by measuring the Mach angle θ in each frame and using the relation $V = C_2^H/\sin\theta$, the propagation speed V was obtained. The average value was 2830 $m/s = 1.10C_1^H = 0.88C_2^S = 0.95C_R^S$. Both methods are found to be in agreement to within 3.2%. The disturbance traveled at a speed approximately 5% lower than the Rayleigh wave speed of steel and 10% lower than the shear wave speed of steel. This result was consistently repeatable. We note that this disturbance is not a generalized Rayleigh wave, since such wave does not exist for bimaterial systems with large contrast in material properties [19–21], such as we have in this case. The photoelastic images do not provide conclusive evidence regarding the exact nature of the disturbance at point A.

The effect of the above disturbance on the process of sliding was deciphered by using the recorded velocity data presented in Fig. 7(b), which shows an expanded view of the history of the velocity of points M_1 and M_2 at the initiation of sliding,. Point M_2, which was on the surface of the steel plate, started moving first at approximately 57.5 μs under the influence of the compressive stress wave propagating in the steel plate. Point M_1 on the Homalite plate started moving at 59 μs. During the following 14 μs, M_1 and M_2 were moving at the same speed until approximately 72 μs. At this time, the point in the steel plate (M_2) decelerated and its velocity became negative. The velocity of the point on the Homalite plate (M_1) followed the same trend after approximately 1.5 μs. Up to this time, there was no sliding, since both points traveled together under the influence of the P-wave in the steel plate, and the relative velocity oscillated around zero. Then, at about 74 μs and 76 μs respectively the velocities of M_1 and M_2 started increasing again. However, in this case, the velocity of the point on the Homalite surface increased faster than the velocity of the point on the steel plate. The corresponding photoelastic frame taken at 75 μs [Fig. 6(b)] shows that a Mach line emanated from the interface, at a short distance in front of the reflective point, and ahead of the P-wave front in the Homalite plate. A very simple calculation shows that a disturbance traveling at a speed of $0.95C_R^S = 1.1C_1^H$ is expected to be at the reflective point at about 74 μs. This confirms that the disturbance caused the increase of the particle velocities. The disturbance was supersonic with respect to Homalite, and therefore, it was ahead

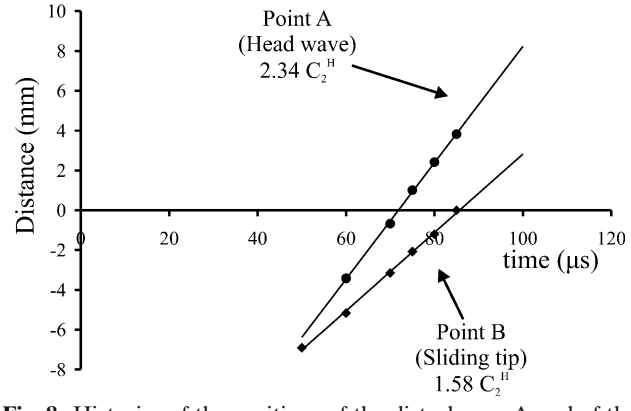

Fig. 8. Histories of the positions of the disturbance A and of the sliding tip B

of the P-wave front traveling in the Homalite plate. In addition, a Mach cone was formed with a tip at the disturbance. The initial impact of the projectile on the steel buffer created a compression P-wave, transmitted into the Homalite plate. Because of friction, some of the energy also transmitted into the steel plate. The P-wave traveled faster in the steel plate than in the Homalite plate, and thus, a precursor effect emerged. Nevertheless, photoelasticity is not very sensitive to compression, and because of this we could not see a possible Mach cone associated with the interface disturbance traveling at the steel P-wave speed. The disturbance, however, caused the photoelastic fringe pattern to warp enough for it to be captured by the high speed camera. The insert in Fig. 6(a) schematically illustrates the loading configuration, the resulting wave fronts, the shear head wave and the supershear sliding tip with the resulting Mach cone. Curves 1, 2 and 3 correspond to the P-wave front in the steel plate, shear wave front in the steel plate and the P-wave front in the Homalite plate. Point A represents the disturbance, just behind the shear wave front in the steel plate, and point B represents the sliding tip.

In Fig. 6(c), the tip of the first Mach line has passed the position of velocity measurement, whereas the eye-like structure has just arrived there. The velocimeter recording shows that at approximately 76 μs the relative horizontal velocity between M_1 and M_2 has increased, but not very sharply. We also note that the numerically calculated relative horizontal displacement between the points M_1 and M_2 was less than 1 μm until 84 μs. This indicates that until 84 μs there was no sliding, but only shear elastic deformation of the material close to the interface (material between M_1 and M_2. Thus, the disturbance and the eye-like fringe structure did not create slip.

However, at approximately 84 μs, a drastic change occurred in the relative velocity and in the relative displacement [see Fig. 7(a)]. The velocity of the measurement point in the Homalite plate increased rapidly, whereas the velocity of the point in the steel plate remained almost constant. This resulted in a very steep rise in the relative velocity and in a very abrupt change in the slope of the relative displacement vs. time diagram. We conclude that the sliding, at the position of measurement, started at around 84 μs. The corresponding photoelastic frame [see Fig. 6(d)] captured at 85 μs is extremely revealing, in which a fringe concentration point [point B of Fig. 6(a) and (b)] coincided with the measurement position. It is the sliding tip, and because it propagated with a supershear speed, a Mach line emanated from this position. Indeed, following the positions of the tip in different frames (see Fig. 8) and using a linear interpolation, we obtained the tip propagation velocity which was 1970 $m/s = 1.58C_2^H$, higher than the shear wave speed of Homalite.

The velocimeter measurement [Fig. 7(a)] shows that the speed increased sharply from 84 μs to approximately 98 μs, and then it remained almost constant until 110 μs, where a second acceleration event happened. The time instance of 98 μs (when the acceleration ceased) corresponded to a fringe concentration point C [see Fig. 6(d)]. After point C, the fringes were parallel to the interface, which means that a constant maximum shear stress field was formed. In Fig. 6(f), captured at 110 μs, the area of the photoelastic pattern with inclined fringes arrived at the measurement position, and this coincided with the initiation of the secondary acceleration caused by the arrival of the reflected waves from the free side of the Homalite plate. From the relative velocity history diagram, we conclude that sliding was continuous during the recording time. This means that sliding occurred in a crack-like mode.

The above exhaustive study of the experimental results clearly shows the power of the proposed point velocity measurement in combination with the full field technique of photoelasticity. We were able to completely identify the different fringe formations in the photoelastic images and explicitly connect them to the changes in sliding velocity. We finally note that, after the initiation of sliding, the in-plane horizontal particle velocity in the steel plate was one order of magnitude lower than the velocity in the Homalite plate. This is true not only for the experiment analyzed above, but for all of the performed experiments using Homalite - steel bimaterial specimens.

The findings of this experiment are similar to results obtained by experiments on crack growth in bimaterials [22–24]. We note that the first observations of intersonically traveling cracks were made in connection with crack propagation along the interface of bimaterial systems [4–9]. The main difference between the experimental setups involved in crack growth experiments and the setup we used for the sliding is as follows: in the case of crack propagation, the Homalite and steel plates were bonded together and a notch was machined along the bond line at one edge. Thus, the resistance to rupture was generated mainly from the bond. In our case, the resistance to sliding was due to the frictional stress between the surfaces of the two plates. We also note that the frictional resistance was not uniform along the interface and not constant with time, since the dynamic compression and the sliding velocity were changing with position and time.

Observation of Wrinkle-Like Pulses

Our goal in this section is to detect possible wrinkle-like pulses propagating along the interface. Preliminary results showed that, as the confining stress decreased and the impact speed increased, a characteristic fringe structure emanated from the interface, behind the sliding tip. The propagation speed of this fringe structure was always between the Rayleigh wave speed and the shear wave speed of Homalite, within an experimental error. The above speed limits are consistent with the theoretically predicted speed limits of the wrinkle-like pulses [10]. Velocimetry was used to obtain the vertical displacement caused by the wrinkle-like pulse related to the mentioned fringe structure and thus to infer any separation of the surfaces in contact occurred during the sliding event. In the experimental result presented in the previous section, the particle velocities in the steel plate were one order of magnitude less than the velocities in Homalite plate. Taking advantage of this fact, we used two velocimeters to record both the horizontal and vertical in-plane components of the velocity at a point on the Homalite plate, very close to the interface (velocimeters 1 and 2 in Fig. 3). We then interpreted our measurements as "sliding" and "opening" speeds by assuming that the steel plate is effectively rigid compared to the Homalite plate.

Figure 9 shows a sequence of six isochromatic fringe patterns depicting the evolution of maximum shear stress contours in the Homalite plate. The confining external stress applied to the bimaterial specimen was 5 *MPa* and the speed of the projectile at impact was 22 *m*/*s*. Figure 10(a) shows the histories of the horizontal and vertical in-plane components of the velocity at points M and N respectively on the Homalite plate. These points were at a distance of 70 *mm* from the impact side of the Homalite plate and at a distance of less than 250 μ*m* from the interface (see Fig. 9). The vertical displacement at point N was obtained by integrating the vertical velocity with time. At 40 μ*s*, the arrival of the P-wave front and the eye-like fringe structure at point M was captured by the high-speed camera [see Fig. 9(a)]. This was fortuitous because we could now combine visual evidence from the photoelastic picture with the recording of the velocimeters. Figure 10(a) shows that at 40 μ*s* the horizontal velocity increased, whereas the vertical velocity became negative, showing that point N moved downward, toward the velocimeter head. The interpretation is clear. Point

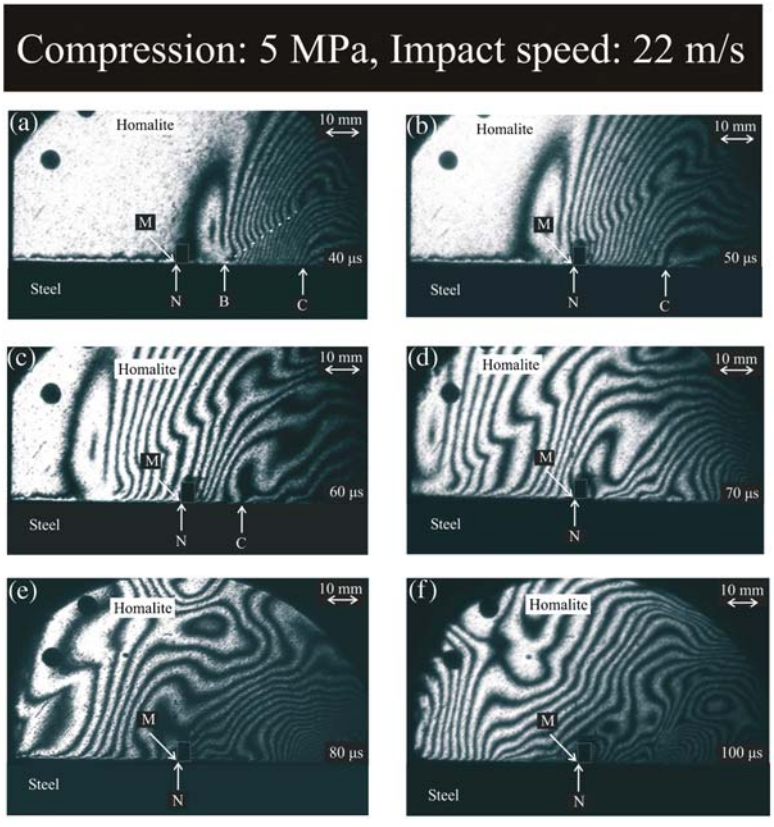

Fig. 9. A sequence of isochromatic fringe patterns showing intersonic frictional sliding, the corresponding shear Mach line (B) and the wrinkle-like pulse (C). The horizontal and vertical in-plane components of the velocity were measured at points M and N respectively

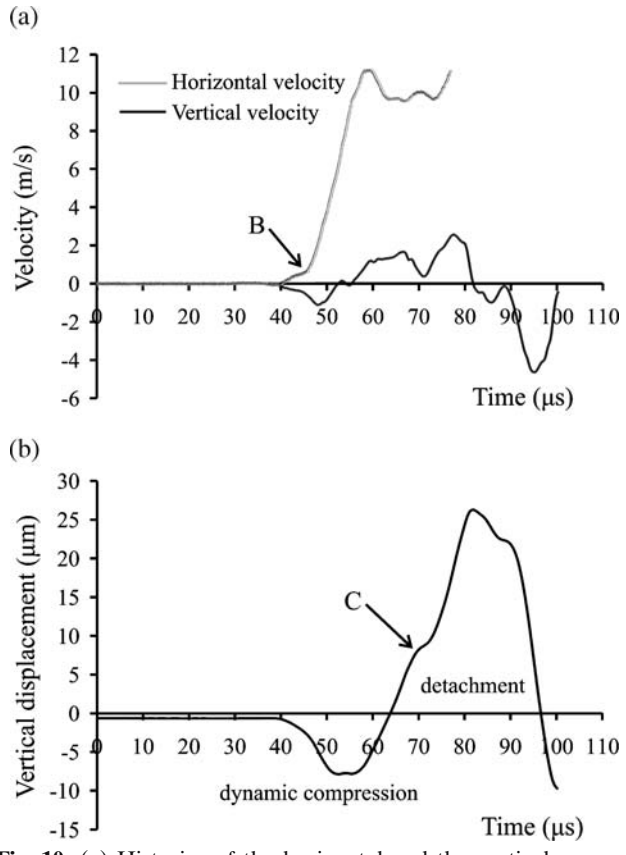

Fig. 10. (**a**) Histories of the horizontal and the vertical components of the in-plane particle velocity measured on the Homalite plate, 70 *mm* from its impact side. The sliding initiated at B. (**b**) History of the vertical displacement

M moved to the left under the influence of the horizontal compressive stress generated by the impact. Because of the Poisson effect, the horizontal compressive stress induced a dynamic (inertial) vertical compressive stress that forced point N to move downward. Using the experience accumulated from the first experiment, we estimated that sliding started at approximately 46 μs, when the relative velocity increased rapidly. From 40 μs to 46 μs, elastic shearing occurred, whereas sliding initiated when the tip of the Mach line [point B in Fig. 9(a)] crossed the velocity measurement position M. At 50 μs, the sliding tip B was on the left of the measurement position Fig. 9(b), signifying that the sliding had already started. Point B was traveling at a supershear speed of 1932 $m/s = 1.55C_2^H$. Figure 10(a) shows that at around 60 μs the horizontal velocity reached its maximum value and the sliding continued for the rest of the recording time with no large variations in the sliding tip speed.

It is interesting to follow the evolution of the vertical velocity in Fig. 10(a), and especially the evolution of the vertical displacement depicted in Fig. 10(b). At the start, the specimen was subjected to a uniform external compression of 5 *MPa*. A very simple 1D calculation showed that the vertical displacement of point N from the initial uncompressed position was less than 1 μm. The impact wave created a dynamic (inertial) compression which added to the static compression and the displacement became more negative. However, after 55 μs, the vertical velocity became positive, which means that point N was moving upward, approaching the initial uncompressed position. At approximately 65 μs, the displacement became positive, signifying the initiation of the detachment of the Homalite plate from the steel plate. At approximately 95 μs, the opening closed and sliding continued again under compression. Looking at the photoelastic images in Fig. 9, we see that at 65 μs a fringe structure (shown by arrow C) approached the measurement position. At 70 μs this structure arrived at N, where an interface opening started. At 100 μs [see Fig. 9(f)], when the opening was closed, the fringe structure had departed from N. The propagation speed of this fringe pattern was 1260 $m/s = 1.0C_2^H$. The data show that the above fringe structure represents a wrinkle-like pulse traveling along the interface. The obtained speed is also consistent with theoretical results, which show that the propagation speed of a wrinkle-like pulse is between the Rayleigh wave and the shear wave of the Homalite [10]. The wrinkle-like pulse has been predicted theoretically and numerically [10–12]. However, this is the first observation of a wrinkle-like pulse at high strain rate experiments on elastic bimaterials. Optical evidence of wrinkle-like pulses traveling along interfaces of similar-material plates have been shown by the same investigators [25]. Anooshehpoor and Brune [13] have found similar wrinkle-like pulses in sliding experiments involving very slow wave speed materials such as foam rubber. The above-mentioned fringe structure appeared in all experiments conducted at high impact speeds and low compressive loads, and was always connected to a local opening. We mention that the wrinkle-like pulse was not present in the first experiment, because the impact speed was not high enough to trigger detachment. Finally, we note that the whole area from point B to point C in Fig. 9(a) was under frictional sliding and compression.

Concluding Remarks

A new technique has been developed to record the evolution of the in-plane components of the particle velocity in real time. The combination of velocimetry with the full-field technique of dynamic photoelasticity was shown to be a very powerful tool in the

study of dynamic frictional sliding along incoherent interfaces.

The experiments involved bimaterial specimens consisting of Homalite-100 and steel plates held together by uniform compressive stress and subjected to impact shear loading. The following significant effects were captured:

- The interaction between the impact wave and the preexisting static stress field caused a relatively broad loading wave that emanated from the interface.
- A disturbance, traveling along the interface at a speed close to the Rayleigh wave speed of steel, generated a Mach line that crossed the P-wave front and the eye-like fringe pattern. Data recorded by the velocimeter showed that this disturbance affected the relative velocity but did not cause sliding.
- The velocimeter revealed that the sliding initiated behind the eye-like fringe structure. A shear Mach line was visible in the photoelastic images, indicating that the sliding was supershear with respect to the shear wave speed of Homalite.
- The sliding occurred in a crack-like mode.
- A self-sustaining wrinkle-like pulse propagating along the bimaterial interface was observed. It caused a local detachment between the two plates that was traveling at a speed close to the Rayleigh wave speed of Homalite. It is expected that the wrinkle-like pulse might play an important role in the failure mechanism of bimaterial structures subjected to impact shear loading.

Acknowledgments The authors gratefully acknowledge the support of the Office of Naval Research through grant N00014-03-1-0435 (Dr. Y.D.S. Rajapakse, Program Manager). The authors would also like to thank "Polytec", USA, (M. Pineda and E. Lawrence), for the use of the second velocimeter.

References

1. Freund LB (1990) Dynamic fracture mechanics. Cambridge, UK.
2. Broberg KB (1999) Cracks and fracture. Academic Press, London.
3. Rosakis AJ (2002) Intersonic shear cracks and fault ruptures. Adv Phys 51(4):1189–1257.
4. Tippur HV, Rosakis AJ (1991) Quasi-static and dynamic crack growth along bimaterial interfaces: a note on crack-tip field measurements using coherent gradient sensing. Exp Mech 31:243–251.
5. Liu C, Lambros J, Rosakis AJ (1993) Highly transient elastodynamic crack growth in a bimaterial interface: higher order asymptotic analysis and optical experiments. J Mech Phys Solids 41(12):1857–1954.
6. Lambros J, Rosakis AJ (1995) Shear dominated transonic interfacial crack growth in a bimaterial-I. Experimental observations. J Mech Phys Solids 43(2):169–188.
7. Singh RP, Shukla A (1996) Subsonic and transonic crack growth along a bimaterial interface. J Appl Mech 63:919–924.
8. Rosakis AJ, Samudrala O, Singh RP, Shukla A (1998) Intersonic crack propagation in bimaterial systems. J Mech Phys Solids 46(10):1789–1813.
9. Kavaturu M, Shukla A, Rosakis AJ (1998) Intersonic crack propagation and interfaces: experimental observations and analysis. Exp Mech 38(3):218–225.
10. Comninou M, Dundurs J (1977) Elastic interface waves involving separation. J Appl Mech ASME 44:222–226.
11. Weertman J (1980) Unstable slippage across a fault that separates elastic media of different elastic constants. J Geophys Res 85:1455–1461.
12. Andrews DJ, Ben-Zion Y (1997) Wrinkle-like slip pulse on a fault between different materials. J Geophys Res 102:553–571.
13. Anooshehpoor A, Brune JN (1999) Wrinkle-like Weertman pulse at the interface between two blocks of foam rubber with different velocities. Geophys Res Lett 23:2025–2028.
14. Abou-Sayed AS, Clifton RJ, Hermann L (1976) The Oblique-plate impact experiment. Exp Mech 16:127–132.
15. Kim K-S, Clifton RJ, Kumar P (1977) A combined normal- and transverse-displacement interferometer with an application to impact of y-cut quartz. J Appl Phys 48(10):4132–4139.
16. Sharpe WN (1971) Interferometric surface strain measurement. Int J Nondestr Test 3:59–76.
17. Sharpe WN, Payne TS, Smith MK (1978) Biaxial laser-based displacement transducer. Rev Sci Instrum 49(6): 741–745.
18. Lu J, Suresh S, Ravichandran G (1998) Dynamic indentation for determining the strain rate sensitivity of metals. J Mech Phys Solids 51(11–12):1923–1938.
19. Achenbach JD, Epstein HI (1967) Dynamic interaction of a layer and a half-space. J Eng Mech 5:27–42.
20. Ranjith K, Rice JR (2001) Slip dynamics at an interface between dissimilar materials. J Mech Phys Solids 49:341–361.
21. Rice JR, Lapusta N, Ranjith K (2001) Rate and state dependent friction and the stability of sliding between elastically deformable solids. J Mech Phys Solids 49:1865–1898.
22. Samudrala O, Rosakis AJ (2003) Effect of loading and geometry on the subsonic/intersonic transition of bimaterial interface crack. Eng Fract Mech 70:309–337.
23. Samudrala O, Huang Y, Rosakis AJ (2002) Subsonic and intersonic mode II crack propagation with a rate-dependent cohesive zone. J Mech Phys Solids 50:1231–1268.
24. Coker D, Rosakis AJ, Needleman A (2003) Dynamic crack growth along a polymer composite-homalite interface. J Mech Phys Solids 51:425–460.
25. Lykotrafitis G, Rosakis AJ (2006) Sliding along frictionally held incoherent interfaces in homogeneous systems under dynamic shear loading. Int J Fract, accepted.